Proceedings of the
Annual Stability Conference
Structural Stability Research Council
San Antonio, Texas, March 19-22, 2024

Developing a concentrated plasticity model for high-strength steel beams with local buckling and member slenderness considerations

Abdullah Alghossoon[1], Amit Varma[2], Duaa Alomoush[3]

Abstract

This paper focuses on the behavior, modeling, and evaluation of high-strength steel beams used as girders in moment-resisting frame systems (MRFs). This study utilizes a fusion of experimental test outcomes, 2D fiber-based simulations and cutting-edge Artificial Intelligence (AI) techniques to develop a concentrated plasticity-based model that includes the effect of local buckling in high-strength steel beams. The key parameters influencing the behavior of high-strength steel beams are: (i) geometric details, (ii) material stress-strain behavior, and (iii) fracture/damage failure criteria. This paper summarizes the experimental data on the monotonic and cyclic behavior of high-strength steel beams to calibrate and validate 2D fiber-based models. Subsequent parametric studies are then conducted to investigate the effects of material and geometric parameters on high-strength steel beams' cyclic behavior and ductility. The Artificial Neural Network (ANN) enriches the dataset, while the Gene Expression Programming (GEP) technique aids in formulating idealized flexure-rotation relationships. These relationships play a crucial role in the potential development of design methods founded upon recently proposed allowable strain criteria and/or continuous strength methodologies by other researchers.

1. Introduction

High-strength steels (HSSs) are structural steels having a nominal yielding strength F_y greater than specified in the current design codes; for instance, 345 MPa is the limit in the AISC 360-22 Specifications (*American Institute of Steel Construction* 2022). Recent steel-making breakthroughs and technical advances have resulted in suitable HSS with enhanced weldability and ductility. HSS constructions provide various advantages, including reduced material use, smaller earthquake response, lower consumption of energy, and more friendly to the environment. Compared to conventional strength steel (CSS), with a nominal yielding strength of less than 525 MPa, HSSs have two distinct features that may result in variable mechanical performances when utilized in structures. First, the stress-strain curves of thermomechanical rolled HSS derived from tension coupon testing show a higher yielding strength to tensile strength (F_y/F_u) ratio but no visible yielding plateau. Second, geometric defects and residual stresses in welded-section

[1] Assistant Professor, Civil Engineering Department, Faculty of Engineering, The Hashemite University, P.O. box 330127, Zarqa 13133, Jordan <abdullahm_ab@hu.edu.jo>
[2] Professor, Purdue University, < ahvarma@purdue.edu >
[3] M.Sc. Student, Civil Engineering Department, Faculty of Engineering, The Hashemite University, P.O. box 330127, Zarqa 13133, Jordan, <2170432@std.hu.edu.jo>

elements made of HSS are thought to have less of an influence on local buckling behavior (Rasmussen and Hancock 1992).

The existing design codes, namely the American Institute of Steel Construction (AISC 360-22) and Eurocode 4 EN1994-1-1 (EC4), do not adequately address the design requirements for HSS flexural members. These codes do not sufficiently capture the unique characteristics and considerations associated with HSS flexural members. Furthermore, when HSS is employed in flexural members, it frequently allows for a reduction in component plate thickness compared to conventional CSS (Compact Shape Section) plates. As a result, the width-to-thickness ratio of HSS component plates is often higher, rendering HSS flexural members more susceptible to local buckling behavior. Limited research has delved into the flexural performance of HSS, considering material properties, loading conditions, geometry, and configurations. McDermott (McDermott 1969) investigated A514 steel I-section beams with a yield strength of 690 MPa, exploring local and overall buckling under varying moment conditions. Lee et al. (Lee et al. 2013) studied flange slenderness impact on HSB800 and HSA800 steel I-section beams (800 MPa yield strength).

High-strength steel's unique characteristics pose challenges due to limited studies compared to conventional steel types (e.g., ASTM A36, A572, A992). Notably, Green (Green, Ricles, and Sause 2001) has extensively investigated the structural ductility of high-strength steel members in his Ph.D. dissertation and subsequent publications. His studies encompassed a range of experiments on welded I-shaped HSLA-80 flexural members, with a focus on the impact of material stress-strain characteristics, cross-sectional geometry, and various loading conditions. Through his experimental investigations, Green observed that the stress-strain characteristics of high-strength steel (HPS) have a significant influence on the inelastic behavior of flexural members, particularly when compared to similar members constructed from mild steel. These findings highlight the importance of understanding and considering the unique stress-strain properties of high-strength steel in assessing the inelastic behavior and rotational ductility of such structural elements. The experimental research conducted by Schillo and Feldmann (Schillo and Feldmann 2017) concludes a rotation capacity of $R = 3$ for specimens made of S700 but lesser values for S970 steel. In addition, the influence of the loading conditions was observed, where the four-point loading beam exhibited greater rotational capacity compared to the three-point loading beam, where strains tend to localize in a more concentrated manner.

Designing structures for seismic resilience involves accounting for inelastic deformations. Therefore, in recent times, there has been a growing inclination towards the development of plasticity models for high-strength steel beams. These models aim to facilitate the utilization of computer-aided static and dynamic analyses, enabling extensive and comprehensive parametric studies. In a related study, Chen et al. (Chen et al. 2014 and Chen et al. 2016) explored the hysteretic behavior of Q690 high-strength steel H-section and box-section beam columns via cyclic loading tests. Wang et al. (Wang et al. 2014) focused on high-strength welded steel beam-column members, developing a trilinear hysteretic model for precise descriptions of cyclic performance under seismic loads. The authors introduced a fiber-based model in their recent study to simulate local buckling effects in high-strength steel beams. Each fiber's stress-strain curve in their model was established through nonlinear regression analysis of a benchmarked 3D finite element (FE) model and fine-tuned using experimental test outcomes. While their 3D FE and 2D fiber-based models address various factors believed to influence behavior, like initial

imperfections, residual stresses, and stress-strain curve attributes, it's computationally expensive and limited to specific computer software featuring fiber-based modeling capabilities.

Artificial Intelligence (AI) has transitioned from computer science to practical applications, demonstrating its transformative potential. For instance, it excels in accurately predicting the behavior of structural systems and components (Alghossoon et al. 2023). This study utilizes two types of AI techniques and builds upon the authors' previous published research by introducing a concentrated plasticity model to simulate the effect of local buckling in HSS beams signifies a pivotal leap forward in seismic structural engineering. This proposed model represents a crucial development, enabling design engineers, within commonly used software platforms to investigate the behavior of seismic force-resisting systems.

2. Methodology

2.1 Methodology in a Nutshell

This study attempts to utilize the authors' previous research outcomes on HSS beams and the most cutting-edge AI techniques for the development of an idealized concentrated plasticity model that considers the effect of local buckling in high-strength steel beams. Such a model can be implemented in most commercial FE software as shown in Fig.1 (b). A large-scale parametric study is established to assess the impact of various geometric parameters (h/b, h/t_w, b/t_f, t_f/t_w) on the moment-rotation behavior of a cantilever HSS beam. The resulting moment rotation curves are normalized to the section flexural strength at yield and simplified using a tri-linear curve. The anchor points in the idealized tri-linear curve represent yielding strength (M_y, Θ_y), peak strength (M_u, Θ_u), and section residual strength (M_R, Θ_R) as denoted in Fig. 1. The mechanism of the proposed anchor points is investigated using the artificial neural network and gene expression programming. Finally, the developed concentrated plasticity model will be validated against experimental tests from the literature using one of the commercial FEM software that includes multi-linear plastic springs/links (such as SAP 2000, ETABS., etc.).

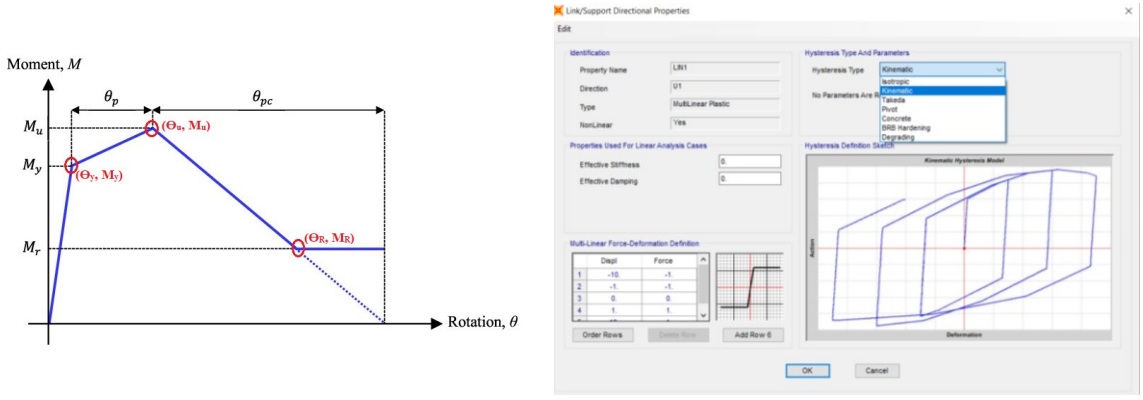

(a) (b)

Figure 1 : (a) The proposed tri-linear moment rotation curve of HSS beams, (b) Multi-linear plastic link in SAP 2000

2.2 Finite element model description

The numerical analysis of the high-strength steel beam in this paper was conducted using the 2D fiber-based model proposed in the authors' prior research (Alghossoon and Varma 2023) as shown

in Fig.2. This model was developed based on extensive experimental and numerical simulation outcomes. The developed effective stress-strain curve shown in Fig. 2 holds the key to developing a useful fiber-based model that takes into account several aspects that are believed to control the high-strength steel beam's cyclic behavior, such as the initial imperfection, residual stresses, material hardening model, and material damage model.

The fiber-based model is implemented in OpenSEES (OS), as shown in Fig. 2 and Table. 1, comprises sub-elements interconnected at the boundaries through cross-section fibers. The choice of the assigned element type is contingent upon the expected behavior and the desired response, encompassing elastic behavior, peak force, and fracture point. In this study, a displacement-based element, typically a Bernoulli-type element, was adopted, following standard finite element procedures to approximate the displacement field for deformation interpolation. To address shear deformation at the end of the beam model, a shear spring was incorporated, as illustrated in Fig. 2. The length of the plastic hinge in the I-shape steel sections can be quite complex, However, it was found that a simple expression yielded a reasonable estimate of the length such that 1.8*b* and 2.5*b* for sections with depth-to-width ratio *h/b* of 1 and 2, respectively. The author adopted the regularization techniques to mitigate mesh sensitivity associated with the use of softening material. This method ensures the maintenance of the same fracture energy dissipation (area under the stress-strain curve) as that of the reference length, representing the physical length of the plastic hinge.

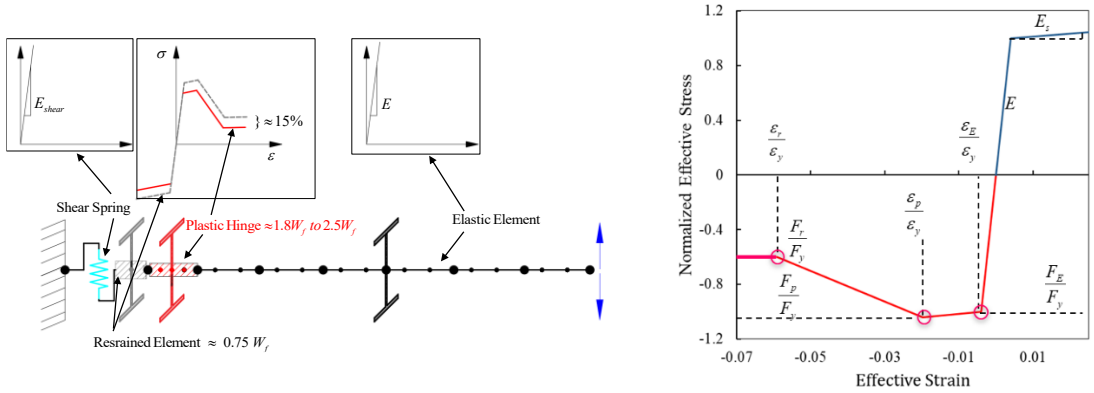

(a) (b)

Figure 2 : (a) Fiber-based model of HSS beam using OpenSEES, (b) Idealized stress-strain curve (Alghossoon and Varma 2023)

Table 1: Normalized stress and strain expression in the fiber-based model (Alghossoon and Varma 2023)

Strain	Stress
$\frac{\varepsilon_r}{\varepsilon_y}=\begin{cases}1.5\varepsilon_p & for\ \varepsilon_p>0.1\\ \begin{cases}\left(\frac{1.75}{\lambda_w^{0.15}\lambda_f}-0.07\right) & for\ \lambda_f<10\\ \left(\frac{1.15}{\lambda_w}+0.058\right)-\frac{1}{\lambda_w^{0.15}\lambda_f} & for\ \lambda_f\geq 10\end{cases} & for\ \varepsilon_p\leq 0.1\end{cases}$	$\frac{F_r}{F_y}=\begin{cases}\max\left(\left(\frac{205}{\sqrt{\lambda_w}}-25\right)\frac{1}{\lambda_f^2}+0.5,\frac{F_p}{F_y}\right) & for\ \varepsilon_p\leq 0.1\\ 0.6 & for\ \varepsilon_p>0.1\end{cases}$
$\varepsilon_p=\max\left(\frac{660}{\lambda_w*\lambda_f^3},2\varepsilon_y\right)$	$\frac{F_p}{F_y}=\begin{cases}\min\left(\left(\frac{120000}{\lambda_w^3\ \lambda_f^2}\right)+1,1.05\right) & for\ \lambda_f\leq 10\\ \frac{100}{\lambda_f^2} & for\ \lambda_f>10\end{cases}$
$\varepsilon_E=\varepsilon_y$	$F_E=F_y$

2.3 Validation of the OpenSEES model

To validate the discussed (OS) modeling, the test results of high-strength steel beams conducted by Shinohara et al. (Shinohara, Suekuni, and Ikarashi 2012), Elkady and Lignos (Elkady and Lignos 2018), Haia et al. (Hai et al. 2019), and Green et al. (Green, Ricles, and Sause 2001) were utilized. The verification process involved comparing the OS model results to the experimental data, considering factors such as material properties, model dimensions, restraining configurations, initial geometric imperfections, and residual stresses, as well as other available test information from the literature. The comparison between the test results and the fiber-based model results is presented in Fig. 3. It was observed that the findings obtained from the fiber-based model exhibited a high level of concurrence with the experimental results, in terms of initial stiffness peak strength, cyclic degradation, and overall behavior.

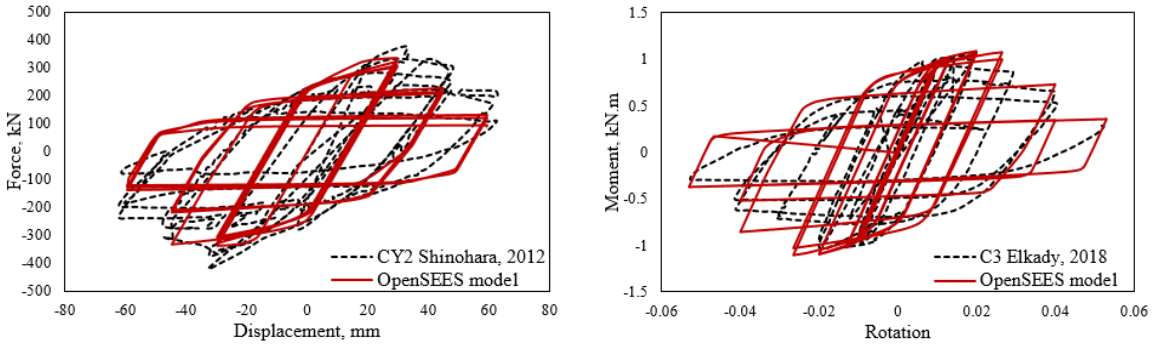

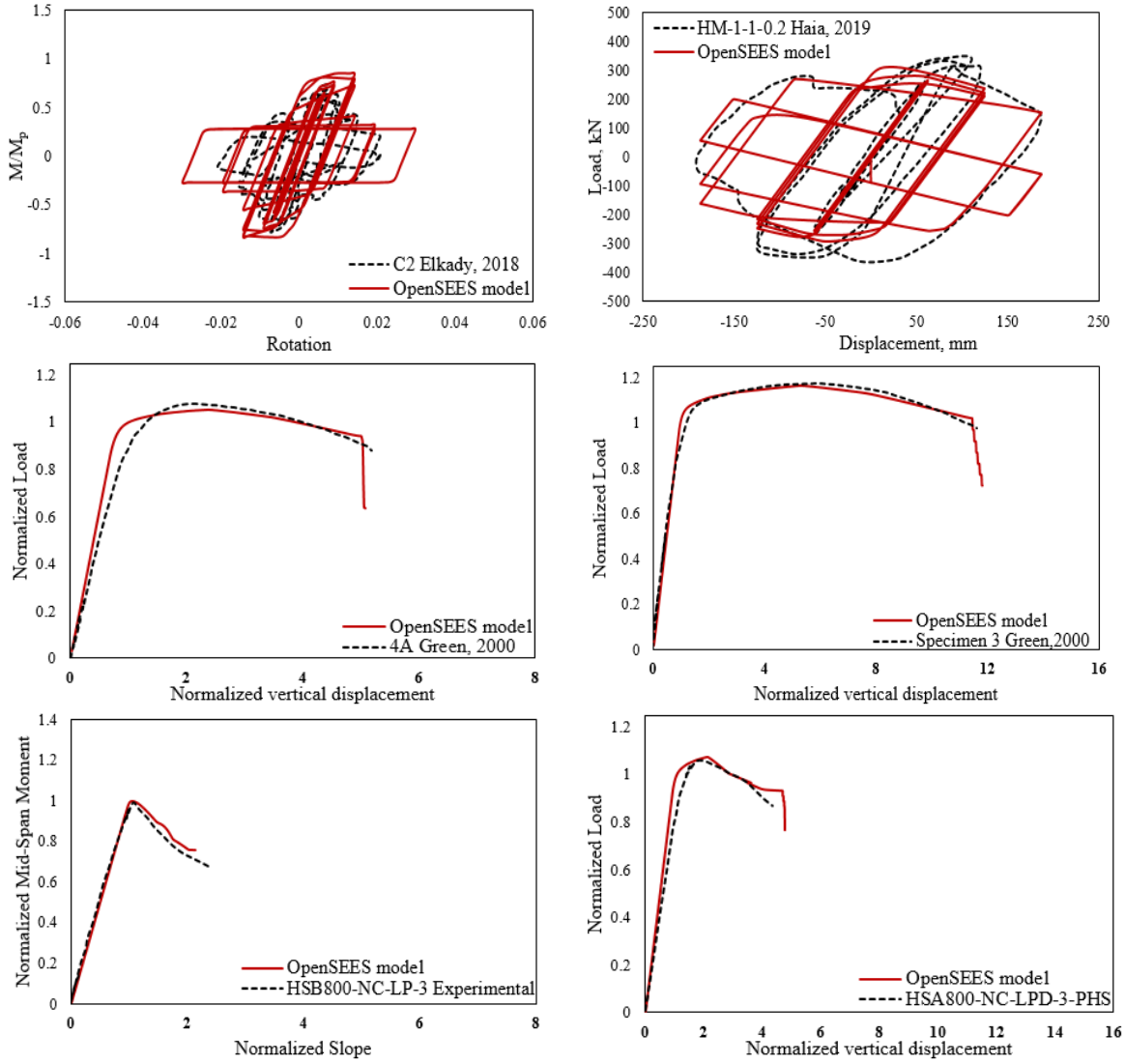

Figure 3 : Comparison between the OS results and experimental tests.

The calibrated 2D fiber-based model of the high-strength steel beam was employed to create a series of steel beam models. These models varied in the flange and web slenderness ratios, aiming to explore how different section shapes affect both the monotonic and cyclic behavior of the beams. The ratio between depth and width in the chosen sections closely resembles the standard US steel sections like W12, W14, and W21. Additionally, it aligns with the recommended slenderness ratio often observed in the built-up sections of conventional buildings. The idealized trilinear curves shown in Fig. 4 are examples of the adopted moment-rotation curve for the selected high-strength steel beams. The coordinate of the three anchor points on the trilinear curve at the compression side of the curve represents the moment at yield, peak flexural strength, and residual section capacity.

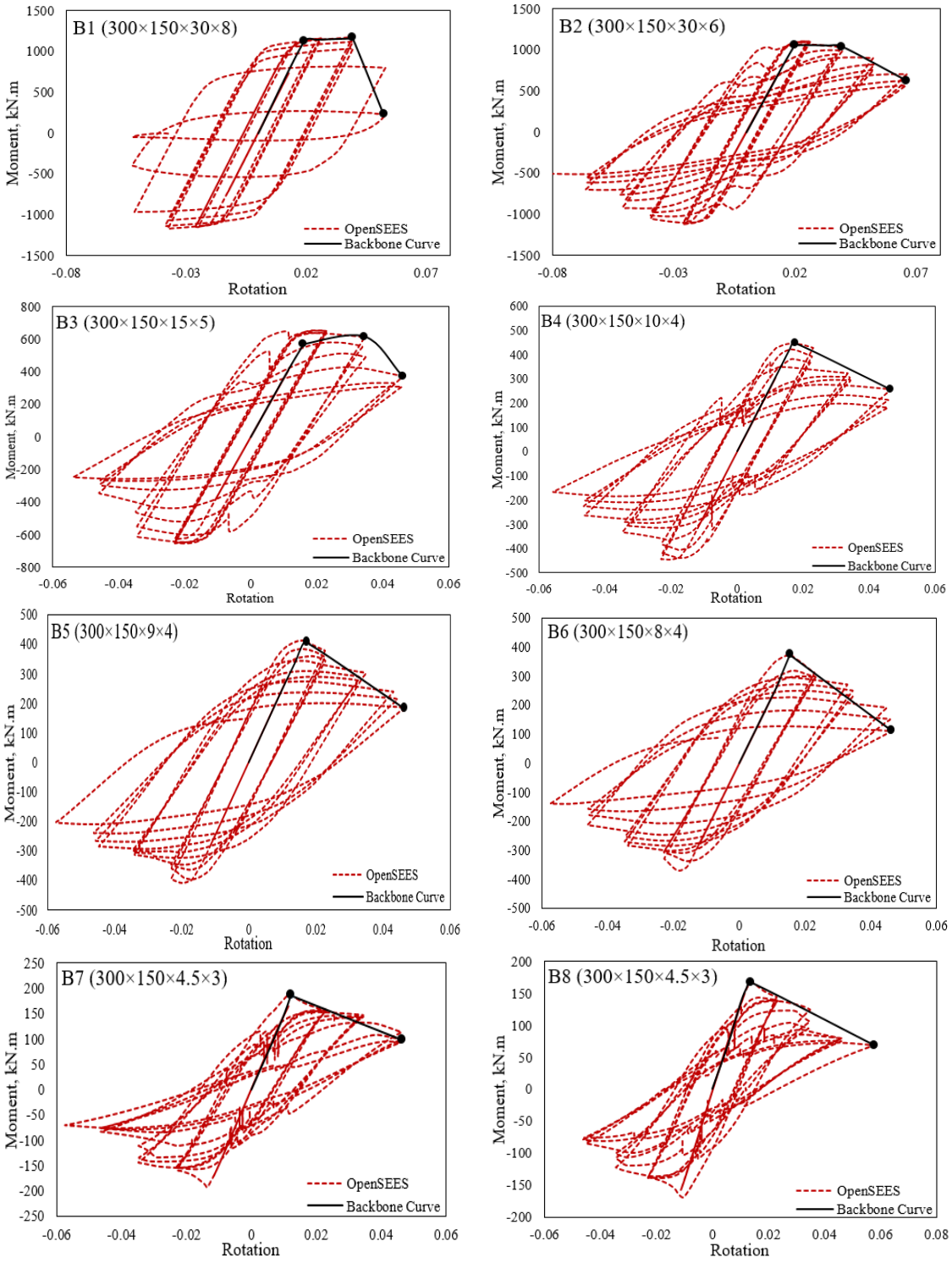

Figure 4 : Idealized back-bone curve of the hysteresis loop from numerical simulations.

2.4 Application of Artificial Intelligence

2.4.1 Artificial Neural Network

Artificial Neural Networks (ANNs) are a relatively new computational tool that has significant applicability in a variety of civil engineering domains. ANNs are highly regarded for their predictive capabilities, enabling them to establish correlations between input variables and associated outputs. Over recent years, numerous researchers have employed ANNs to tackle intricate challenges in structural engineering. For instance, Mallela and Upadhyay (Mallela and Upadhyay 2016) utilized ANNs to forecast the buckling load of laminated composite stiffened panels subjected to in-plane shear loading. Alghossoon et al. (Alghossoon et al. 2023) utilized different AI techniques to predict the shear strength of circular concrete-filled tube members. Dwairi and Tarawneh (Dwairi and Tarawneh 2022) used ANNs to estimate inelastic displacement ratios in structures constructed on soft soils. Similarly, Asteris and Mokos (Asteris and Mokos 2020) employed ANNs to predict concrete compressive strength. Previous studies have concluded that the Artificial Neural Network (ANN) model has remarkable capabilities in predicting structural behaviors, optimizing designs, and facilitating decision-making processes.

The architecture of an ANN generally comprises many layers, including an Input Layer, a Hidden Layer, and an Output Layer as shown in Fig.5. Each layer is made up of interconnected processing units where signals or inputs (x_i) are multiplied by weight values (w_{ji}) and added to bias values (B_{ji}) at each unit (Eq.1). The combined inputs (I_j) are then passed through a nonlinear transfer function $f(I_j)$ to produce the processing outputs, which serve as inputs for the subsequent layer. In this study, a hyperbolic tangent transfer sigmoid function is employed. It is a common practice to separate the dataset into 80% for training the model and 20% for testing and validation. The ANN model is trained using the Levenberg-Marquardt optimization approach, which adjusts the input weights and bias values to minimize the mean square error (MSE) and achieve optimal performance. A combination of squared errors and weights is minimized during the training process, employing Bayesian regularization. The training continues until the MSE converges, indicating no further improvement.

$$I_j = \sum w_{ji}\, x_i + B_{ji} \tag{1}$$

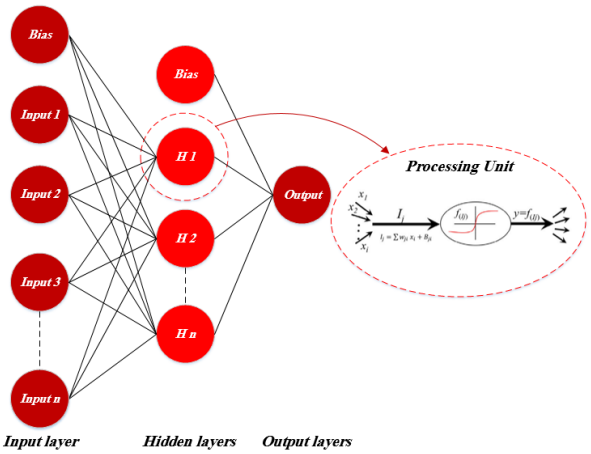

Figure 5 : General structure and processing unit of ANNs.

2.4.2 Integrating Gene Expression Programming (GEP) in Structural Engineering Applications
At its core, GEP operates as an evolutionary algorithm inspired by the principles of genetic evolution. It mirrors biological gene expression through an iterative process that evolves mathematical expressions by encoding them as chromosomes and refining them across successive generations. Its versatility spans various domains such as optimization, modeling, and pattern recognition, positioning it as a promising tool in computational intelligence. In the realm of structural engineering analysis, the utilization of advanced computational tools has seen a significant surge. GEP emerges as a potent methodology, offering a robust approach to model complex relationships between input parameters and structural responses such as the bond strength of fiber-reinforced polymer and concrete (Quayyum 2010), predicting the ultimate axial strain of FRP-confined concrete (Mansouri et al. 2018) and the shear strength of slender RC beams without shear reinforcement (Gandomi et al. 2014).

Gene Expression Programming (GEP) functions by encoding potential solutions to problems into strings of genes organized within chromosomes, like the human analogy and the mechanisms of gene expression. Initially, a population of chromosomes is created randomly, encompassing a combination of functions, terminals, and variables. These chromosomes undergo expression, where their genes assemble into mathematical expressions typically structured in a tree format. An assessment against a predetermined fitness function indicates the efficacy of these mathematical expressions. The selection of the best fitness chromosomes via an iterative procedure evolves through the action of three basic genetic operators to generate new individual chromosomes, namely; Reproduction (copies chromosomes without any modification), Crossover (the exchange of genetic material), and Mutation (the introduction of random alterations). This iterative evolutionary process persists across numerous generations, refining the solutions within the population until predefined termination conditions, such as achieving a particular fitness threshold or completing a designated number of generations, are fulfilled. Ultimately, the program demonstrates the highest performance solution found in the final population.

Fig. 6 represents the five core elements in GEP: (1) Function shape that describes mathematical operations used in gene expressions, guiding how variables are manipulated. (2) The peripheral group that represents structural parameters like material properties or dimensions in equations. (3) Evaluates how well gene expressions predict structural behavior, using metrics like RMSE. (4) Control of variables that manage which parameters influence models, focusing analysis on critical factors. (5) Stopping criteria. Figure. 6 shows the GEP algorithm used to generate the expression tree (Murad 2021).

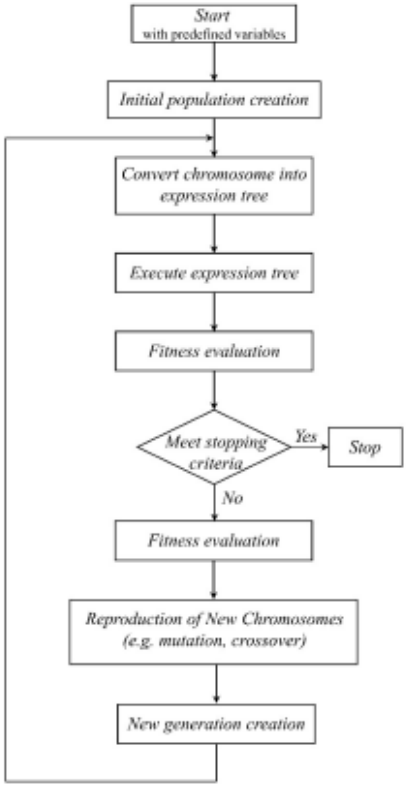

Figure 6 : Gene expression algorithm.

The initial step in the algorithm is to select the five items mentioned previously. The initial functions are generated at random using the function form and terminals given. The method is continued for a certain number of generations or until a satisfactory categorization rate is obtained. The functions that were constructed are then executed and turned into a tree structure. Following that, the fitness function is used to evaluate the results of the functions created; if the results are acceptable, the process is ended. The result is represented in the form of tree structures. These trees, known as GEP expression trees, enable the explanation of mathematical functions created in an easy-to-read format as shown in Fig. 7.

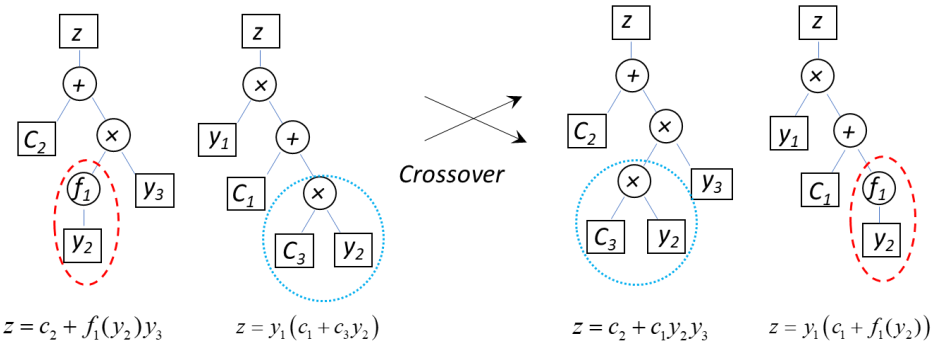

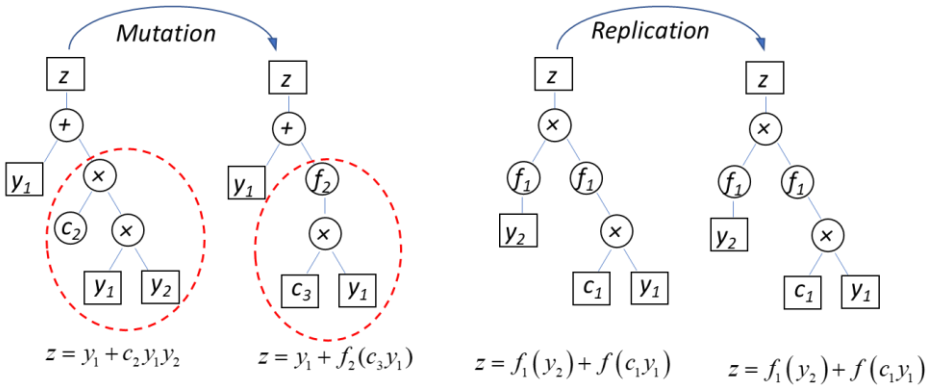

Figure 7 : Mathematical expression and basic genetic operators in Gene expression tree

3. Conclusion

In conclusion, this study presents a robust approach to developing a concentrated plasticity model for high-strength steel beams, accounting for local buckling and member slenderness considerations. This study investigated the monotonic and cyclic behavior of the high-strength steel beam leveraging a calibrated 2D fiber-based model and artificial intelligence techniques, specifically Artificial Neural Networks and Gene Expression programming. The primary aim of this study is to provide a comprehensive and user-friendly model, accessible for engineers in design offices and researchers within commonly used commercial FEM software to simulate the local buckling behavior of high-strength steel beams.

4. Future work

The establishment of the concentrated plasticity model using AI technique is currently under investigation and will be proposed in the next research paper. The assessment of the high-strength steel beam compactness limit and ductility will be investigated in future work.

References

Alghossoon, Abdullah, Ahmad Tarawneh, Ghassan Almasabha, Yasmin Murad, Eman Saleh, Hamza Abu Yahia, Abdallah Abu Yahya, and Haitham Sahawneh. 2023. "Shear Strength of Circular Concrete-Filled Tube (CCFT) Members Using Human-Guided Artificial Intelligence Approach." *Engineering Structures* 282 (May): 115820. https://doi.org/10.1016/j.engstruct.2023.115820.

Alghossoon, Abdullah, and Amit H. Varma. 2023. "Fiber-Based Model for Simulating Strength and Stiffness Deterioration of High-Strength Steel Beams." *Thin-Walled Structures* 183 (February): 110432. https://doi.org/10.1016/j.tws.2022.110432.

American Institute of Steel Construction. 2022. "AISC 360-22 Specifications for Structural Steel Buildings," 2022.

Asteris, Panagiotis G., and Vaseilios G. Mokos. 2020. "Concrete Compressive Strength Using Artificial Neural Networks." *Neural Computing and Applications* 32 (15): 11807–26. https://doi.org/10.1007/s00521-019-04663-2.

Dwairi, Hazim M., and Ahmad N. Tarawneh. 2022. "Artificial Neural Networks Prediction of Inelastic Displacement Demands for Structures Built on Soft Soils." *Innovative Infrastructure Solutions* 7 (1): 1–15. https://doi.org/10.1007/s41062-021-00604-y.

Elkady, Ahmed, and Dimitrios G Lignos. 2018. "Full-Scale Testing of Deep Wide-Flange Steel

Columns under Multiaxis Cyclic Loading: Loading Sequence, Boundary Effects, and Lateral Stability Bracing Force Demands." *Journal of Structural Engineering* 144 (2): 4017189.
Gandomi, Amir H., Amir H. Alavi, Sadegh Kazemi, and Mostafa Gandomi. 2014. "Formulation of Shear Strength of Slender RC Beams Using Gene Expression Programming, Part I: Without Shear Reinforcement." *Automation in Construction* 42: 112–21. https://doi.org/10.1016/J.AUTCON.2014.02.007.
"Gene Expression Programming Application for Prediction of Ultimate Axial Strain of FRP-Confined Concrete." 2018. *Elektronički Časopis Građevinskog Fakulteta Osijek*, July, 64–76. https://doi.org/10.13167/2018.16.6.
Green, Perry S., James M. Ricles, and Richard Sause. 2001. "The Inelastic Behavior of High Performance Steel Flexural Members." In *Proceedings - Annual Technical Session, Structural Stability Research Council*, 261–90.
Hai, Le-Tian, Guo-Qiang Li, Yan-Bo Wang, Fei-Fei Sun, and Hua-Jian Jin. 2019. "Experimental Investigation on Cyclic Behavior of Q690D High Strength Steel H-Section Beam-Columns about Strong Axis." *Engineering Structures* 189: 157–73.
Lee, Cheol-Ho, Kyu-Hong Han, Chia-Ming Uang, Dae-Kyung Kim, Chang-Hee Park, and Jin-Ho Kim. 2013. "Flexural Strength and Rotation Capacity of I-Shaped Beams Fabricated from 800-MPa Steel." *Journal of Structural Engineering* 139 (6): 1043–58. https://doi.org/10.1061/(asce)st.1943-541x.0000727.
Mallela, Upendra K., and Akhil Upadhyay. 2016. "Buckling Load Prediction of Laminated Composite Stiffened Panels Subjected to In-Plane Shear Using Artificial Neural Networks." *Thin-Walled Structures* 102: 158–64. https://doi.org/10.1016/j.tws.2016.01.025.
McDermott, John F. 1969. "Plastic Bending of A514 Steel Beams." *Journal of the Structural Division* 95 (9): 1851–71.
Murad, Yasmin Zuhair. 2021. "Predictive Model for Bidirectional Shear Strength of Reinforced Concrete Columns Subjected to Biaxial Cyclic Loading." *Engineering Structures* 244: 112781.
Quayyum, Shahriar. 2010. "Bond Behaviour of Fibre Reinforced Polymer (FRP) Rebars in Concrete." *Master Thesis*, no. June: 1–169.
Rasmussen, Kim J R, and Gregory J Hancock. 1992. "Plate Slenderness Limits for High Strength Steel Sections." *Journal of Constructional Steel Research* 23 (1–3): 73–96.
Schillo, Nicole, and Markus Feldmann. 2017. "The Rotational Capacity of Beams Made of High-Strength Steel." *Proceedings of the Institution of Civil Engineers: Structures and Buildings* 170 (9): 641–52. https://doi.org/10.1680/jstbu.16.00119.
Shinohara, Takuma, Ryota Suekuni, and Kikuo Ikarashi. 2012. "Cyclic Behavior of High Strength Steel H-Shaped Beam." *Applied Mechanics and Materials* 174–177: 159–65. https://doi.org/10.4028/www.scientific.net/AMM.174-177.159.
Wang, Yan-Bo, Guo-Qiang Li, Wei Cui, and Su-Wen Chen. 2014. "Seismic Behavior of High Strength Steel Welded Beam-Column Members." *Journal of Constructional Steel Research* 102: 245–55.